2nd URSI AT-RASC, Gran Canaria, 28 May - 1 June 2018

Advances in Target Conformal SAR Deposition For Hyperthermia Treatment Planning

Gennaro G. Bellizzi[(1)(2)], Martina T. Bevacqua[(1)], Giada M. Battaglia[(1)], Lorenzo Crocco[(2)] and Tommaso Isernia[(1)(2)]
(1) DIIES, Università Mediterranea di Reggio Calabria, Reggio Calabria, Italia,
{gennaro.bellizzi, martina.bevacqua, giada.battaglia, tommaso.isernia}@unirc.it
(2) CNR-IREA, Consiglio Nazionale delle Ricerche, Napoli, Italia, *crocco.l@irea.cnr.it*

Abstract

The possibility of uniformly shaping the SAR deposition over a target area while avoiding normal tissue to be undesirably heated represents one of the main open challenges in hyperthermia treatment planning. This task is even more challenging when dealing with large targets generally characterized by irregular shapes. Two innovative SAR shaping strategies, aimed at addressing the above-mentioned need, have been recently proposed. These strategies take advantage from the use of more *target points* and are respectively based on two well-known focusing techniques. In this communication, both the approaches are firstly given under a common mathematical framework and then tested on anatomically and electromagnetically realistic phantoms.

1 Introduction

Hyperthermia is a cancer treatment modality which consist in taking the tumor temperature to a supra-physiologic temperature ($40-44^{\circ}C$) for 60-90min. Its actual benefits and effectiveness have been clinically shown and this has taken this cancer treatment modality to be under the way of being considered as a first line treatment in combination with radio- and chemo-therapy. However, accurate and real-time strategies able to control the administered heating still represent a crucial steps for further progress and a widespread clinical adoption of hyperthermia [1]. In this respect, hyperthermia treatment planning (HTP) plays a central and fundamental role.

Treatment planning consists in optimally designing the complex excitation coefficients driving the phased array applicator in order to deliver to the patient a target conformal specific absorption rate (SAR) distribution, i.e., “uniform" within the target area while avoiding undesired heating of the surrounding healthy tissues. So far, many efforts were focused in developing strategies able to focus the electric field within the target area [1]. However, uniformly shape the SAR within an extended target areas (possibly with irregular contours) while keeping it curbed in the healthy tissues, still represents an open challenge, as this task is generally not achieved by means of the conventional strategies aimed at *just* focusing the SAR into a given point within the target area. Very recently two different (but still with many similarities) approaches able to deal with extended target areas have been proposed. In place of a single target point, both these techniques take advantage from a set of target points, say *control points*, placed within the target area, and are based respectively on two focusing techniques: the focusing via constrained power optimization (FOCO) [2] and the time reversal (TR) [3].

A straightforward possibility would suggest to tackle the shaping problem by simply solving the focusing problem, either with FOCO or TR, and then juxtapose the results, named in following “independent" multi-target FOCO (i-mt-FOCO) and TR (i-mt-TR), respectively. On the other side, doing that one is neglecting an additional degree of freedom of the problem which is represented by the phase shifts of the field in the different control points. In particular by exploiting this variable, both the so called multi-target FOCO (mt-FOCO) [4] and the multi-target TR (mt-TR) [5] are able to sensibly improve performances with respect to i-mt-FOCO and i-mt-TR. In the specific, both mt-FOCO and mt-TR address the shaping problem spanning different values of the phase shifts and a-posteriori picking the most convenient one.

Despite aimed at a common end, different aspects are singularly characterizing these two approaches. From one side, mt-FOCO delivers the globally optimal solution as it casts the shaping problem as several convex programming (CP) problems[1] and it exploits a so-called mask function able to enforce arbitrary constraints on power deposition outside the target volume, enabling *hot-spots* avoidance. On the other side, differently from the previous approach, mt-TR is not able to enforce constrains on the power deposition outside the target area, as this represents an intrinsic limitation of TR, but it has a relatively modest computational burden since it “only" requires a linear superpositions for each considered phase shift value.

In this work, for the first time, mt-FOCO and mt-TR are reported in a common mathematical background, tested in a 2D anatomically and electromagnetically realistic breast phantoms and the results benchmarked to the standard “unoptimized" approaches.

[1] One for each considered phase shift value.

By sake of simplicity, we will refer here to the case of scalar fields (deferring some comments the case of vector field to the Conclusion). This is the case of electromagnetic fields when one component can be considered dominant above the other ones [6]. Also note we deal herein with monochromatic fields.

2 The Proposed Approaches

Let Ω be a generic 3-D region of interest surrounded by N elementary monochromatic electric sources. Indicating with $\Phi_n(\underline{r})$ the total scalar field induced by the unitary excited n-th antenna in Ω when all the other antennas are off, the overall field in a generic point of $\underline{r} \in \Omega$ can be expressed as:

$$E(\underline{r}) = \sum_{n=1}^{N} I_n \Phi_n(\underline{r}) \tag{1}$$

where $I_n (n = 1,2,...,N)$ is the set of complex excitation coefficients.

Let us consider a set of *control points*, say $\underline{r}_{t\,i}$ $(i = 1,..,L)$, "arbitrary" located into the target area. By the sake of simplicity, let us refer to the case of just two control points and let $\phi \in [-\pi, \pi]$ be an auxiliary variable indicating the phase shift between the fields in $\underline{r}_{t\,1}$ and $\underline{r}_{t\,2}$.

2.1 Multi-Target FOCO

Starting from the focusing formulation of FOCO, as in [2], the constrained shaping problem can be formulated as:

Find I_n $(n = 1,...,N)$ *such to:*

$$max\left\{ \sum_{j=1}^{2} \Re\{E(\underline{r}_{t\,j})\}^2 + \Im\{E(\underline{r}_{t\,j})\}^2 \right\} \tag{2.a}$$

subject to:

$$\left|E(\underline{r}_{t\,1})\right| = \left|E(\underline{r}_{t\,2})\right| \tag{2.b}$$

$$\left|E(\underline{r})\right|^2 \leq \mathscr{M}\mathscr{F}(\underline{r}) \qquad \underline{r} \in \Omega \setminus \Pi(\underline{r}_t) \tag{2.c}$$

Where the *"mask"* function $\mathscr{M}\mathscr{F}(\underline{r})$ is a non-negative arbitrary function enforcing patient-specific constraints on the power deposition outside the chosen focal area, $\Pi(\underline{r}_t) \in \Omega$.

This formulation (2) is able to guarantee both the uniformity of the field at the target points and the avoidance of unwanted heating, respectively enforcing constrains (2.b) and (2.c). This formulation is non-linear and belongs to the class of the NP-hard problems [4]. However, similarly to FOCO, we can assume the field in $\underline{r}_{t\,1}$ to be purely real which simply changes the overall phase reference of the system. Further, exploiting the redundancy of (2.a) and (2.b), and taking advantage from the additional degrees of freedom represented by the auxiliary variable ϕ, problem (2) is conveniently recast as:

For sufficiently sampling values of ϕ*, determine* I_n *such to:*

$$max\left\{ \Re\{E(\underline{r}_{t\,1})\} \right\} \tag{3.a}$$

subject to:

$$\Im\{E(\underline{r}_{t\,1})\} = 0 \tag{3.b}$$

$$\Re\{E(\underline{r}_{t\,2})\} = \Re\{E(\underline{r}_{t\,1})\} cos(\phi) \qquad \phi \in [-\pi, \pi] \tag{3.c}$$

$$\Im\{E(\underline{r}_{t\,2})\} = \Re\{E(\underline{r}_{t\,1})\} sin(\phi) \qquad \phi \in [-\pi, \pi] \tag{3.d}$$

$$\left|E(\underline{r})\right|^2 \leq \mathscr{M}\mathscr{F}(\underline{r}) \qquad \underline{r} \in \Omega \setminus \Pi(\underline{r}_t) \tag{3.e}$$

Where constraints (3.c) and (3.d) still enforce the uniformity of the field in the target points.

For any fixed value of ϕ, problem (3) is cast as the maximization of a linear function in a convex set, which corresponds to a CP problem [4]. As such, mt-FOCO is able to determine the globally optimal solution by solving different CP problems and then *a-posteriori* picking the most convenient one, f.i. the one maximizing cost function (3.a). For more details the reader is referred to the end of Sect. 2.2 and to [4].

2.2 Multi-Target Time Reversal

Denoting with $\Psi_n(\underline{r}_{t\,i})$ the total field measured by the *n-th* antenna when a unit amplitude point source is located into the control point $\underline{r}_{t\,i}$, according to the standard TR theory, the focused field in $\underline{r}_{t\,i}$ would be provided by:

$$E_i(\underline{r}) = \sum_{n=1}^{N} \Psi_n^*(\underline{r}_{t\,i}) \Phi_n(\underline{r}) \tag{4}$$

where the subscript $*$ denotes the conjugation operation.

By sake of a better understanding, a first multi target version of TR, the so-called i-mt-TR [7], would be given by a linear sum of the excitations corresponding to different control points, so that:

$$I_n = \Psi_n^*(\underline{r}_{t\,1}) + \Psi_n^*(\underline{r}_{t\,2}) \tag{5}$$

Starting from this formulation, the mt-TR approach, for each (sampled) value of ϕ, casts the shaping problem as the combination through complex unit amplitude coefficients, of the fields focused in correspondence of $\underline{r}_{t\,1}$ and $\underline{r}_{t\,2}$ through TR. The excitations coefficients could be determined as:

$$I_n = \Psi_n^*(\underline{r}_{t\,1}) + \Psi_n^*(\underline{r}_{t\,2}) e^{j\phi} \tag{6}$$

Analogously to mt-FOCO, the optimal solution can be efficiently determined by observing a-posteriori the results achieved at the different ϕ values, and picking the most convenient one according with the application at hand.

A possibility is selecting amongst the different $\phi-$solutions the one providing the best trade off between the field intensity distribution closest to the desired one within the

target area and the lowest side peak elsewhere. Alternatively, a simpler possibility, which is the one adopted in the following, consists in selecting the *optimal* ϕ as the one maximizing the sum of the SAR in the control points, i.e., $\sum_{i=1}^{L} \sigma \left| E(\underline{r}_{ti}) \right|^2 / \rho$.

The generalization to the case of L control points and M sampled values of the auxiliary variables will require M^{L-1} linear superpositions for the mt-TR whereas CPs for the mt-FOCO. Note, one can take profit from parallel computing.

3 Numerical Test Bed

The test-bed used in this study is made up by 2-D breast phantoms derived from the anatomically and electromagnetically realistic 3-D phantoms provided by Wisconsin repository [8]. The phantoms are representative of three virtual patients characterized by different fatty and fibroglandular tissue compositions, say cases **A**, **B** and **C** respectively. The original phantoms are referred to healthy patients and therefore an elliptical inclusion, of dimension $\approx 3\lambda_{bg}/2 \times \lambda_{bg}/4$[2], simulating a tumor has been inserted in the breast model. Tumor dielectric properties have been set accordingly to the literature adopting a single-pole Debye dispersion characteristic [9].

The breast is supposed to be surrounded by a matching and/or cooling liquid aimed at both reducing the reflection at the breast surface and keeping the skin temperature curbed. The relative permittivity and the conductivity of the background medium have been set equal to 18 and $0.1 S/m$, respectively, accordingly with [10].

The applicator is supposed to be a circular array of elementary (filamentary) currents surrounding the breast phantom with a radius $\approx 14cm$. The number of array elements has been set equal to 25 accordingly to the theory of Degrees of Freedom [11]. The working frequency is $1,25 GHz$ accordingly to [2], considered the best trade-off between penetration depth and resolution.

4 Results: Analysis and Discussion

Figure 1 reports for both of the analyzed cases the normalized SAR distribution obtained by means of mt-FOCO and mt-TR. In order to get the desired shaping, three control points have been used and have been arranged uniformly (with a spacing of $\approx 0.4\lambda_{bg}$) along a segment along the main axis of the target area. Besides what can be straightforward appreciated by the results depicted, in order to have quantitative metrics, the following analysis has been carried out considering synthetic HTP parameters. These are the target coverage 25% (TC25), as in [12], which was shown to be predictive for clinical outcome for hyperthermia [13], and the maximum SAR level in healthy tissues, say SAR Side Peak (SSP).

[2]Being λ_{bg} the wavelength in the background medium.

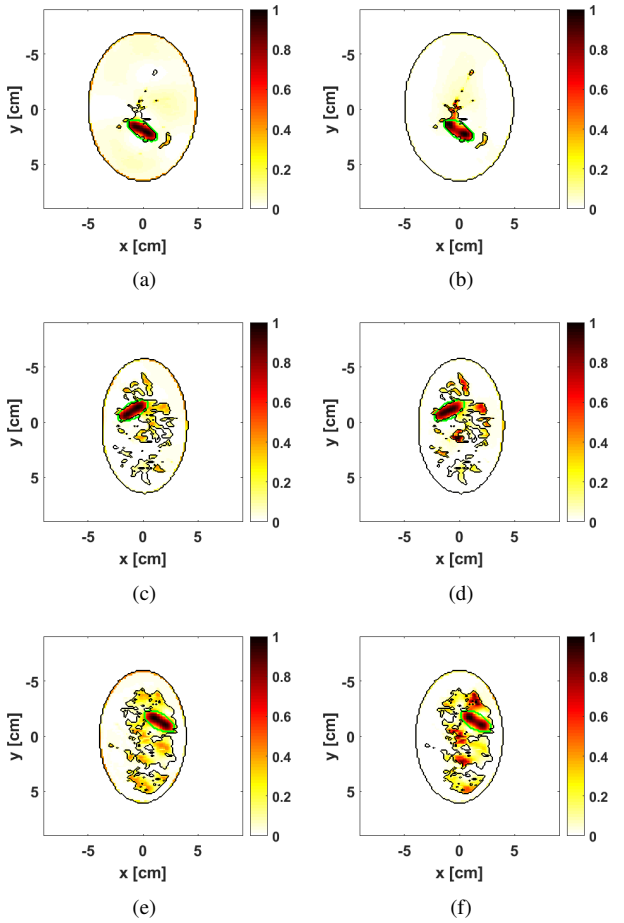

Figure 1. Normalized SAR distributions achieved by means of mt-FOCO and Omt-TR (1^{st} and 2^{nd} column respectively) for cases **A**, **B** and **C** (1^{st}, 2^{nd} and 3^{rd} row respectively).

Table 1 reports the synthetic metrics in addition to the visual information provided by Fig. 1. First, as expected, mt-FOCO outperforms the i-mt-FOCO by an absolute % gain of $\approx 35\%$ in terms of TC25 and, similarly mt-TR does with i-mt-TR by $\approx 25\%$. Second, SSP values related to the TR-based shaping approaches are sensibly higher than the FOCO ones as no constrains can be enforced. Last, it is worth to note that similar TC25 values are achieved by means of both mt-FOCO and mt-TR.

5 Conclusions

In this communication, both mt-FOCO and mt-TR has been presented under a common mathematical background and tested on anatomically and electromagnetically realistic 2D phantoms. The results, benchmarked to the existing standard strategies, show the effectiveness of the proposed approaches.

Current activities have a twofold aim. First, as the applicability of the technique is presently limited to the case of a moderate number of control points, efforts are devoted to find more effective procedures for a-priori optimal phase

shifts selection. This will result in keeping the computational burden curbed and consequently simplifying the procedure when dealing with vector fields (which can be developed by taking into account [14]). Second, this preliminary feasibility assessment lied the basis for a further application of the presented strategies on clinical HTP data.

Acknowledgment

This work has been supported by the Italian Ministry of Research under PRIN Field and Temperature Shaping for MWI Hyperthermia *FAT SAMMY*. This work is relevant to both COST Actions MiMed TD1301 and EMF-MED BM1309.

References

[1] M. M. Paulides, G. M. Verduijn, and N. V. Holthe, "Status quo and directions in deep head and neck hyperthermia," *Radiation Oncology (2016) 11:21*, 2016, DOI 10.1186/s13014-016-0588-8.

[2] D. A. M. Iero, T. Isernia, and L. Crocco, "Thermal and Microwave Constrained Focusing for Patient-Specific Breast Cancer Hyperthermia: A Robustness Assessment," *IEEE Antennas Propagat. Trans.*, vol. 62, pp. 814–821, 2014.

[3] T. J. L., F. Wu, and M. Fink, "Time reversal focusing applied to lithotripsy," *Ultrason. Imaging*, vol. 18, pp. 106–121, 1996.

[4] G. G. Bellizzi, D. A. M. Iero, L. Crocco, and T. Isernia, "Towards 3D Intensity Shaping:The Scalar Case," *IEEE Antennas and Wireless Propagation Letter*, 2017.

[5] G. G. Bellizzi, L. Crocco, and T. Isernia, "Spatial Field Intensity Shaping via Optimized multi target Time Reversal," in *32nd URSI GASS, Montreal, 19-26 August 2017*, 2017.

[6] P. Togni, Z. Rijnen, W. Numan, R. Verhaart, J. Bakker, G. van Rhoon, and M. M. Paulides, "Electromagnetic redesign of the HYPERcollar applicator: toward improved deep local head-and-neck hyperthermia," *Phys Med Biol.*, no. 58(17), pp. 5997–6009, 2013.

[7] D. Zhao and M. Zhu, "Generating Microwave Spatial Fields with Arbitrary Patterns," *IEEE Antennas and Wireless Propagation Letters*, no. 99, pp. 1–4, 2016.

[8] E. Zastrow, S. K. Davis, M. Lazebnik, F. Kelcz, B. D. V. Veen, , and S. C. Hagness, "Database of 3D grid-based numerical breast phantom for use in computational electromagnetics simulations," *[Online]. Available: http://uwcem.ece.wisc.edu/home.htm*.

[9] C.Gabriel, S.Gabriel, and E.Corthout, "The dielectric properties of biological tissues: I. Literature survey," *Phys. Med. Biol.*, vol. 41, pp. 2231–2249, 1996.

Table 1. Synthetic HTP parameters of the considered analysis

	A		B		C	
	TC25 [%]	SSP [%]	TC25 [%]	SSP [%]	TC25 [%]	SSP [%]
mt-FOCO	81	42	81	41	96	38
i-mt-FOCO	50	46	51	40	53	45
mt-TR	79	78	79	100	93	94
i-mt-TR	48	80	59	88	67	93

[10] I. Catapano, L. D. Donato, L. Crocco, O. Bucci, A. Morabito, T. Isernia, and R. Massa, "On quantitative microwave tomography of female breast," *Progress in Electromagnetic Research*, vol. 97, pp. 75–93, 2009.

[11] O. M. Bucci and T. Isernia, "Electromagnetic inverse scattering: retrievable information and measurement strategies," *Radio Sci.*, vol. 32, pp. 2123–2137, 1997.

[12] R. Canters, P. Wust, J. Bakker, and G. V. Rhoon, "A literature survey on indicators for characterisation and optimisation of SAR distributions in deep hyperthermia, a plea for standardisation," *International Journal of Hyperthermia*, vol. 25, no. 7, pp. 593–608, 2009.

[13] H. Lee, A. Antell, C. Perez, W. Straube, G. Ramachandran, and R. M. et al., "Superficial hyperthermia and irradiation for recurrent breast carcinoma of the chest wall: Prognostic factors in 196 tumors," *Int J Radiat Oncol Biol Phys*, vol. 40, pp. 365–75, 1998.

[14] D. A. M. Iero, "Constrained Power Focusing in Inhomogeneous Media as a Polarization Optimization," *International Journal of Antennas and Propagation, Article ID 705819,*, 2015.